Inhibitors of Metallo-β-lactamase Generated from β-Lactam Antibiotics †

ARTICLE *in* BIOCHEMISTRY · JULY 2005

Impact Factor: 3.02 · DOI: 10.1021/bi050302j · Source: PubMed

5 AUTHORS, INCLUDING:

Adriana Badarau
Newcastle University
23 PUBLICATIONS **310** CITATIONS
SEE PROFILE

Antonio Llinas
AstraZeneca
43 PUBLICATIONS **667** CITATIONS
SEE PROFILE

Andrew Peter Laws
University of Huddersfield
58 PUBLICATIONS **1,095** CITATIONS
SEE PROFILE

Michael I Page
University of Huddersfield
205 PUBLICATIONS **4,559** CITATIONS
SEE PROFILE

Articles

Inhibitors of Metallo-β-lactamase Generated from β-Lactam Antibiotics†

Adriana Badarau,‡ Antonio Llinás,‡ Andrew P. Laws,‡ Christian Damblon,§ and Michael I. Page*,‡

Department of Chemical and Biological Sciences, University of Huddersfield, Queensgate, Huddersfield HD1 3DH, U.K., and Biological NMR Centre, Medical Sciences Building, University of Leicester, Leicester LE1 9HN, U.K.

Received February 18, 2005; Revised Manuscript Received April 29, 2005

ABSTRACT: The resistance of bacteria to the normally lethal action of β-lactam antibiotics is largely due to the production of β-lactamases that catalyze the hydrolysis of the β-lactam. One class of these enzymes is a zinc-dependent metallo-β-lactamase for which there are no clinically available inhibitors. The hydrolysis of cephalosporin β-lactam antibiotics generates dihydrothiazines which subsequently undergo isomerization at C6 by C−S bond cleavage and through the intermediacy of a thiol. These thiols can be trapped by the β-lactamase from *Bacillus cereus*, causing inhibition of the enzyme. The rate of production of the thiol corresponds to the rate of inhibition, and the inhibition constants are in the micromolar range but vary with the nature of the cephalosporin derivative. NMR studies have identified the structure of the thiols causing inhibition and also show that the thiol binds to the zinc ion, which in turn perturbs the metal-bound histidines. Inhibition is slowly removed as the thiol becomes oxidized or undergoes further degradation. The thiol intermediate generated from cephalothin is a slow binding inhibitor. There is no observed inhibition from the analogous degradation products from penicillins.

β-Lactamases inactivate β-lactam antibiotics, such as penicillin (**1**), by catalyzing the hydrolysis of the four-membered ring (Scheme 1), and these enzymes play a major role in the emergence of pathogenic bacteria that are resistant to these important antibacterial agents (*1*). The β-lactamases that contain an active site serine residue, which acts as a nucleophile to attack the β-lactam carbonyl carbon (classes A, C, and D), have been extensively studied (*1*). However, the class B β-lactamases or metallo-β-lactamases (MBLs)[1] are metalloenzymes that require zinc ion for their activity and are less well understood (*2*). The first metallo-β-lactamase to be discovered was produced by an innocuous strain of *Bacillus cereus*, but in the last 20 years, MBL-mediated resistance has appeared in several pathogenic strains and is being rapidly spread by horizontal transfer, involving both plasmid and integron-borne genetic elements (*3*).

Metallo-β-lactamases use one or possibly two zinc ions as cofactors and are capable of hydrolyzing a large variety

Scheme 1

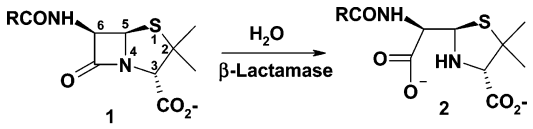

of β-lactam antibiotics including third generation cephalosporins and carbapenems. They have been classified into three groups according to their amino acid sequences (*4*). Subclass B1 is the largest and contains three well-studied β-lactamases: BcII from *B. cereus* (*5*, *6*), CcrA from *Bacteroides fragilis* (*7*−*9*), and IMP-1 from *Pseudomonas aeruginosa* (*10*, *11*). The most common enzyme of subclass B2 is CphA from *Aeromonas hydrophila*, which differs from other MBLs regarding zinc dependence and substrate profile (*12*). Finally, subclass B3 contains the only known tetrameric zinc β-lactamase, the L1 enzyme from *Stenotrophomonas maltophilia* (*13*), although tetramerization is not shared by other members of this subclass (*14*).

The structures of several MBLs have been determined by X-ray diffraction and all, BcII (*5*, *15*), CcrA (*7*, 16), IMP-1 (*11*), L1 (*17*), FEZ-1 (*18*), CphA (*19*), and BlaB (*20*), show a similar αββα fold and two potential zinc ion binding sites at the active site often referred to as sites 1 and 2 (*21*, *22*). The zinc ligands in the two sites are not the same and are not fully conserved between the different MBLs. In the subclass B1 enzymes (*4*) such as the *B. cereus* enzyme BcII the zinc in site 1 (the histidine site) is tetracoordinated by the imidazole of three histidine residues (116, 118, and 196) and a water molecule. In site 2 the metal is pentacoordinated by histidine 263, aspartic acid 120, cysteine 221, and one water molecule; the fifth ligand at site 2 is carbonate (*15*)

† This research was supported by the European Union research network on metallo-β-lactamases within the Training and Mobility of Researchers (TMR) Program, Contract HPRN-CT-2002−00264, and the University of Huddersfield.

* To whom correspondence should be addressed: phone, +1484 472169; fax, +1484 472182; e-mail, m.i.page@hud.ac.uk.

‡ University of Huddersfield.

§ University of Leicester.

[1] Abbreviations: MBL, metallo-β-lactamases; BcII, *Bacillus cereus* β-lactamase II; NMR, nuclear magnetic resonance; PAC spectroscopy, perturbed angular correlation spectroscopy; MOPS, 3-(*N*-morpholino)-propanesulfonic acid; DSS, 3-(trimethylsilyl)-1-propanesulfonic acid; NMWL, nominal molecular weight limit; DTNB, 5,5′-dithiobis(2-nitrobenzoic acid) (Ellman's reagent); HEPES, *N*-(2-hydroxyethyl)-piperazine-*N*′-2-ethanesulfonic acid; DTT, 1,4-dithio-DL-threitol; BSA, bovine serum albumin.

10.1021/bi050302j CCC: $30.25
Published on Web 05/27/2005

or water (*5*, *7*, *16*, *21*) but is missing in one structure (*23*) and in structures with inhibitors bound (*11*). The two metal ions are relatively close to each other, but the distance between them varies from 3.4 to 4.4 Å in different structures of the BcII and CcrA enzymes (*5*, *7*, *11*, *15*, *16*, *21*). Several structures of the CcrA enzyme show a bridging water ligand between the two metals, which is thought to exist as a hydroxide ion (*7*, *21*). In a structure of BcII containing two zinc ions determined at pH 7.5 there is also a similar bridging water molecule (*23*), but in structures of this enzyme at lower pH this solvent molecule is strongly associated to the zinc in site 1 (*5*, *21*). The coordination and geometry of the metal ions are thus quite variable.

X-ray structures obtained in the presence of inhibitors (*11*, *21*, *24*) have suggested several important interactions between subclass B1 enzymes and their substrates (*25*) such as that between (i) the β-lactam carbonyl oxygen with the first zinc ion and the side chain of a well-conserved asparagine, (ii) the substrate carboxylate and the second zinc ion, and (iii) substituents of substrates attached to the β-lactam α-carbonyl carbon and a hydrophobic pocket.

In the majority of MBLs, zinc can be exchanged with cadmium to yield catalytically active enzymes (*6*). The use of a combination of NMR and PAC spectroscopy to study cadmium binding to *B. cereus* MBL has revealed a rapid intramolecular exchange of the metal between the two sites in the monocadmium enzyme and negative cooperativity in metal binding (*26*).

Inhibitors of the class A serine β-lactamases, such as clavulanic acid, have been very widely used to protect penicillins from β-lactamase-catalyzed hydrolysis. However, MBLs are resistant to serine β-lactamase inactivators, and the search for a clinically useful inhibitor of MBLs remains a desirable objective. A number of compounds have been synthesized and investigated as inhibitors of MBLs such as trifluoromethyl alcohols and ketones (*27*), hydroxamates (*28*), thiols (*29*−*33*), including cysteinyl peptides (*34*), thioester derivatives (*30*, *35*, *36*), biphenyl tetrazoles (*37*), thiocarboxylates (*33*), succinic acid derivatives (*24*), tricyclic natural products (*38*), and sulfonyl hydrazones (*39*). Some of the thiol inhibitors of BcII show stereochemical preferences which was rationalized by assuming that the thiol of the inhibitor binds to the active site zinc (*30*). Thiomandelic acid (α-mercaptophenylacetic acid) is a broad-spectrum and reasonably potent inhibitor of MBLs (*33*), and structure−activity relationships show that the thiol is essential for activity, and it was postulated that the inhibitor thiol binds to the zinc ion.

There have been several suggestions regarding the catalytic mechanisms of both the mono- and dizinc forms of the enzymes (*2*). We have shown that the pK_a of the water bound to zinc in BcII is 5.8 and is therefore ionized at neutral pH and that there is a need for a second catalytic group to be ionized, thought to be Asp−120 (*30*). In the mononuclear enzyme, the hydroxide ion bound to zinc has been proposed to be the nucleophile responsible for β-lactam hydrolysis (*30*), whereas in the binuclear version, it is the bridging hydroxide ion (*2*). However, the precise role of the two metals in catalysis remains unclear; mechanisms have been proposed in which only the histidine site zinc plays a direct role in catalysis (*30*) or in which the two zinc ions are both involved as a binuclear center (*2*, *17*, *40*).

Scheme 2

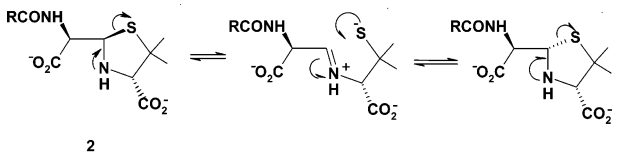

2

The normal hydrolysis product of β-lactam antibiotics is the result of opening the four-membered ring to give the corresponding β-amino acid **2** (Scheme 1). In penicillins this hydrolysis is followed by a much slower reversible ring opening of the five-membered thiazolidine ring, resulting in epimerization at C5 by rapid ring closure of the thiolate−iminium ion intermediate (Scheme 2) (*41*). In cephalosporins **3**, β-lactam ring opening to give the 3,6-dihydro-2*H*-1,3-thiazine derivatives **4** can be followed by expulsion of a leaving group from C3′ to generate an α,β-unsaturated imine **5** (Scheme 3). The latter can subsequently undergo Michael addition by nucleophiles to regenerate derivatives of the initially formed enamine **6**. These hydrolysis products also can undergo a slower epimerization at C6, again by reversible ring opening of the six-membered dihydrothiazine and formation of a thiolate−iminium ion intermediate **7** (Scheme 3) (*42*).

Given the known ability of thiols to inhibit class B β-lactamases, we were interested in exploring the possibility of the enzyme trapping the intermediate thiols using the molecular recognition provided by the basic β-lactam antibiotic substrate structure.

EXPERIMENTAL PROCEDURES

Materials. Reagents used in all kinetic experiments were of analytical grade; cephaloridine and cephalothin were supplied by Glaxo Smith Kline. Cephalexin was purchased from Sigma and used without further purification. Deionized pure water was used for preparation of buffers and other aqueous solutions. Phosphate and MOPS buffers were prepared just prior to the experiment, and potassium chloride was used to maintain a constant ionic strength.

Enterobacter clocae P99 β-lactamase (Speywood, Maidenhead, England) was obtained in powder form and dissolved in 0.1 M MOPS before use. *B. cereus* 569/H/9 (BcII metallo-β-lactamase) was prepared as an aqueous suspension in 10 mM HEPES buffer as previously described (*15*).

Equipment. pH Measurements used a Φ40 pH meter (Beckman, Fullerton, CA) with a calomel glass electrode (Beckman). NMR experiments used a 400 MHz instrument (Bruker). UV spectrometry was carried out on a Cary 1E UV−visible spectrometer equipped with a 12-compartment cell block thermostated by using a peltier system (Varian).

Inhibition Studies. For BcII-catalyzed hydrolysis experiments, 2 mL of buffer solution (0.1 M MOPS, pH = 7.0, I = 1 M, 30 °C, $[Zn^{2+}] = 5 \times 10^{-5}$ M, unless otherwise stated) was equilibrated in the thermostated cell block of the UV spectrophotometer. To this solution was added the desired concentration of enzyme and inhibitor, either together, if they had been incubated with each other, or separately, followed by the substrate. Hydrolysis of the substrate was followed by measuring the decrease in absorbance at 260 nm for cephaloridine, cephalothin, and cephalexin and at 235 nm

Scheme 3

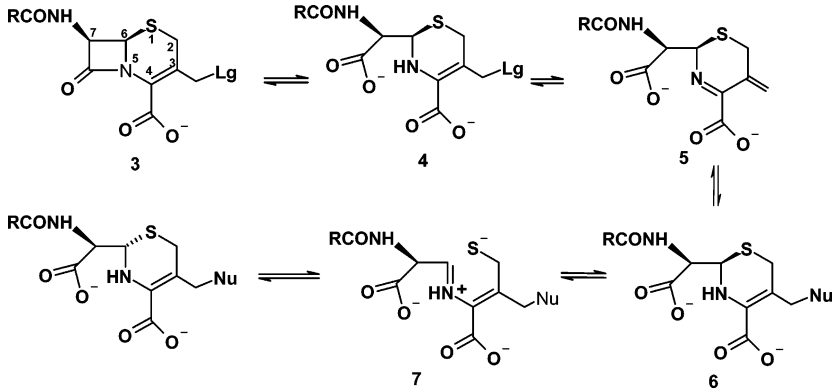

for benzylpenicillin and the increase in absorbance at 490 nm for nitrocefin.

The kinetic constants were generally measured by following the entire course of the reaction. Rate constants were estimated by using Cary Win UV kinetics application Version 02.00 (*26*).

Preparation of Cephaloridine, Cephalexin, and Cephalothin Hydrolysis Products at pH = 7, Enzymatically, Using E. clocae P99 β-Lactamase. To 0.6 mL of 10^{-2} M cephalosporin (0.1 M MOPS, pH = 7.0, I = 1 M, 30 °C) was added 6 μL of a 10^{-4} M stock solution of *E. clocae* P99 β-lactamase, and the mixture was left for about 10 min at 30 °C until the hydrolysis of the antibiotic was complete. The enzyme was then removed from the mixture by centrifugal ultrafiltration using a Microcon (Millipore) centrifugal filter device, with a YM-10 (green top) −10000 NMWL sample reservoir.

Estimation of Kinetic Parameters for Slow Binding Inhibition. The model used for treating cephalothin degradation product inhibition of BcII (Scheme 4) was that proposed by Morrison and Walsh (*43*) for the action of slow binding inhibitors.

The progress curves of BcII-catalyzed hydrolysis of nitrocefin, P, in the presence of cephalothin degradation product were fitted to the equation:

$$P = v_s t + (v_0 - v_s)(1 - e^{-kt})/k \quad (1)$$

where v_0, v_s, and k represent respectively the initial velocity, the final steady-state velocity, and the apparent first-order rate constant for the establishment of equilibrium between EI and EI* and are defined by the equations:

$$v_0 = \frac{V_{max}S}{S + K_m(1 + I/K_i)} \quad (2)$$

$$v_s = \frac{V_{max}S}{S + K_m(1 + I/K_i^*)} \quad (3)$$

$$k = k_{-4}\left[\frac{1 + \frac{I}{K_i^*(1 + S/K_m)}}{1 + \frac{I}{K_i(1 + S/K_m)}}\right] \quad (4)$$

where $K_i = k_{-3}/k_3$ is the dissociation constant of the EI complex and K_i^* is the overall dissociation constant:

$$K_i^* = k_{-4}K_i/(k_{-4} + k_4) \quad (5)$$

Scheme 4

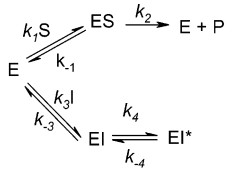

The assumptions involved in using this model are as follows: ES reaches the steady-state instantaneously; k_1S, k_{-1}, k_3I, and k_{-3} are much greater than k_4 and k_{-4}; $k_{-4} < k_4$ and the depletion of the free substrate is negligible.

The progress curves of nitrocefin hydrolysis were recorded at 30 °C in 0.1 M MOPS buffer, pH = 7.0, I = 1 M, $[Zn^{2+}] = 5 \times 10^{-5}$ M, in the presence of different concentrations of cephalothin degradation product, obtained after 6 h incubation in 0.1 M MOPS buffer, pH = 7.0, as described previously. The reaction was initiated by the addition of enzyme (0.25 nM) to a mixture of nitrocefin (75 μM) and cephalothin degradation product (no preincubation); 50 μg/mL BSA was added in the assay cell solution to minimize the denaturation of BcII present at low concentrations.

v_0, v_s, and k were determined by fitting the progress curves to eq 1 for each inhibitor concentration, using SCIENTIST (Micromath Scientific Software) software. Plots of $1/v_0$ and $1/v_s$ against inhibitor concentration gave K_i and K_i^*, respectively (eqs 2 and 3). The value of k_{-4} was determined by fitting the dependency of k on I to eq 4, with SCIENTIST, using the K_i and K_i^* values previously obtained, and k_4 was calculated from eq 5. V_{max} and K_m were calculated by fitting directly the initial rates to the Michaelis−Menten equation.

Determination of Thiol Concentration Using Ellman's Reagent. Ellman's reagent [5,5′-dithiobis(2-nitrobenzoic acid) (DTNB)] stock solution (20 μL, 10^{-2} M) in dioxane was injected into 2 mL of 0.1 M MOPS, I = 1 M, at 30 °C. To this solution was added 20 μL of a 10^{-2} M stock solution of cephalosporin hydrolysis product, and the increase in absorbance was measured at 412 nm, corresponding to the release of 3-carboxy-4-nitrothiophenolate anion. The extinction coefficient of this anion, determined by calibration with L-captopril, is 13500 M^{-1} cm^{-1}, and the thiol concentration in the assay cell was calculated using the Lambert−Beer law (*44*).

NMR Spectroscopy. ^{1}H NMR spectra were recorded on a Bruker AMX-400 spectrometer using an initial cephalosporin concentration of 1×10^{-2} M in deuterated buffer (phosphate, MOPS). The ionic strength was kept constant, 0.5 M, by means of potassium chloride. pD values were taken as pH

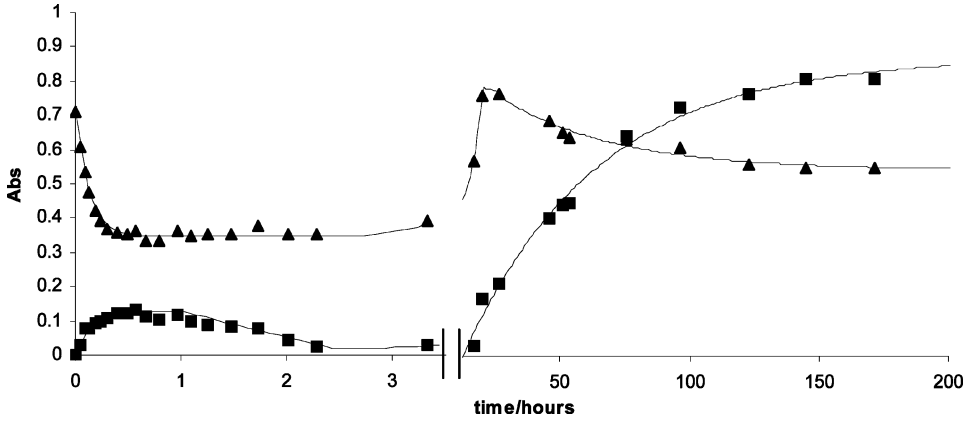

FIGURE 1: Variation of UV absorbance at 260 nm (▲) and 331 nm (■) of 10^{-2} M cephalexin incubated in 0.1 M NaOH and then diluted (100-fold), at various times, into 0.1 M MOPS, pH 7.0. The solid lines represent the sequential first-order fit of the experimental data points. Standard deviations are below 10%.

Scheme 5

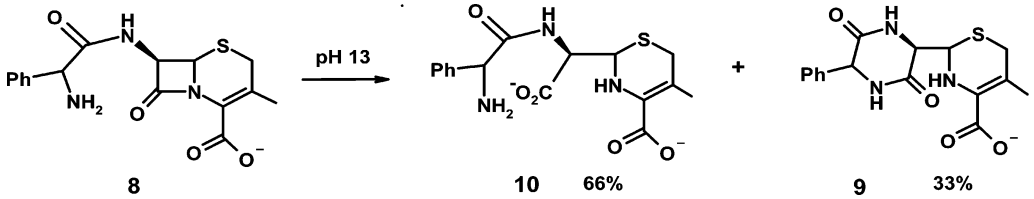

meter readings + 0.40. The buffer solutions and the NMR core were thermostated at 30 °C; the temperature in the NMR spectrometer was calibrated by measuring the shift difference between the CH_2 and the OH peaks (Δ) of a recently prepared sample of 100% ethylene glycol using the equation $T = (4.637 - \Delta)/0.009967$ as in the VT-Calibration Manual (Bruker Instruments). To some of the solutions was added 0.5 mg of P99 β-lactamase. The degradation reactions were also studied in H_2O. Samples were taken at adequate time intervals, frozen with liquid nitrogen, and freeze-dried and the spectra recorded. The sample tube diameter was 5 mm, and 3-(trimethylsilyl)-1-propanesulfonic acid (DSS) was used as internal reference. Chemical shifts are in parts per million. The spectroscopic data obtained were similar to those given by previous authors (*42*, *45*, *46*, *47*).

^{15}N,^{1}H experiments were performed on a Bruker Avance DMX-600 instrument, and long-range $^{15}N(C)H$ correlations detected by $^{1}H-^{15}N$ HMQC (heteronuclear multiple quantum coherence) with a refocusing delay of 16.7 ms ($^1/_2J_{N(C)H}$) were used to observe the histidine imidazole rings as described previously (*26*). The ^{15}N NMR experiments of the complex between the ^{15}N-labeled BCII and cephalexin degradation product were carried out by adding 150 μL of neutralized 10^{-2} M cephalexin degradation product, obtained in 0.1 M NaOH, to 1 mL of 1 mM BCII solution in pH = 7.1, 0.01 M HEPES, 0.1 M NaCl, and 0.005 mM Zn^{2+} at 298 K.

RESULTS AND DISCUSSION

(i) Hydrolysis and Degradation of Cephalexin. The degradation of cephalexin (**8**) in water as a function of time can be monitored by a change in its UV spectrum at 260 and 331 nm (Figure 1) and by NMR.

The degradation route of cephalexin in aqueous solution depends markedly upon pH (*45*). From pH 7 to pH 9 the major product results from intramolecular aminolysis (**9**) whereas in 0.1 M sodium hydroxide there is competitive hydrolysis so that the ratio of normal hydrolysis (**10**) to aminolysis product is 2:1 (Scheme 5). The enzyme-catalyzed hydrolysis of cephalexin (**8**) by both serine and metallo-β-lactamases yields the hydrolysis product (**10**) only. It was possible to compare the effectiveness of the inhibitory properties of the two different products, that from intramolecular aminolysis, the diketopiperazine (**9**), and that from normal hydrolysis (**10**). The intramolecular aminolysis product of cephalexin (**9**) was prepared as described previously (*45*), and the hydrolysis product of cephalexin (**10**) was obtained enzymatically using P99 serine β-lactamase.

Aliquots (20 μL) of a stock solution of cephalexin (10^{-2} M) were incubated in 0.1 M sodium hydroxide and then, at various times, injected into 2.0 mL of MOPS buffer (0.1 M), pH 7.0, containing *B. cereus* 569/H/9 class B metallo-β-lactamase (BcII) (10^{-8} M) and nitrocefin (10^{-5} M) to monitor enzyme activity. It was found that the measured activity of the enzyme was dependent on the length of time cephalexin had been incubated in the sodium hydroxide solution (Figure 2) and the amount added (not shown). For example, after 20 h incubation in sodium hydroxide solution, the mixture of hydrolysis (**10**) and intramolecular aminolysis (**9**) products from 10^{-4} M cephalexin causes complete loss (>98%) of enzyme activity. However, after 1 week of incubation, the solution of degradation products caused no loss of enzyme activity. Incubation of cephalexin in aqueous sodium hydroxide produces an inhibitor of BcII within 1 h. The degree of enzyme activity, after the addition of degradation products (1×10^{-4} M total), as a function of the time cephalexin had been incubated in 0.1 M sodium hydroxide is shown in Figure 2. Variation of the concentration of degradation product added indicated that inhibition was competitive with an apparent K_i of 0.4 μM, determined after 28 h, at $[Zn^{2+}] = 1$ μM. This inhibition constant represents a minimum indication of the potency of the inhibitors because it is calculated on the assumption that all of the cephalexin

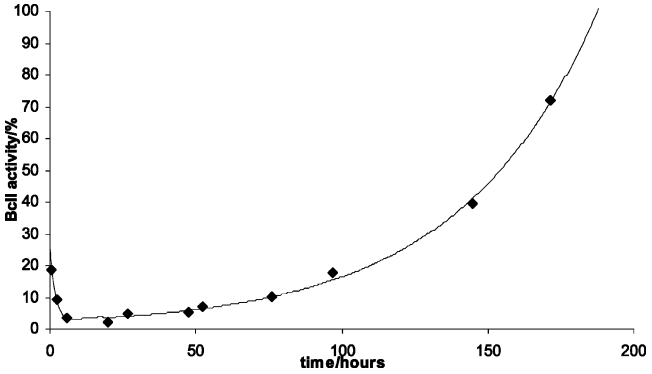

FIGURE 2: Variation of BcII activity, after the addition of 10^{-4} M cephalexin degradation product, as a function of the time cephalexin has been incubated in 0.1 M aqueous sodium hydroxide. The solid lines represent the sequential first-order fit of the experimental data points. Standard deviations are below 10%.

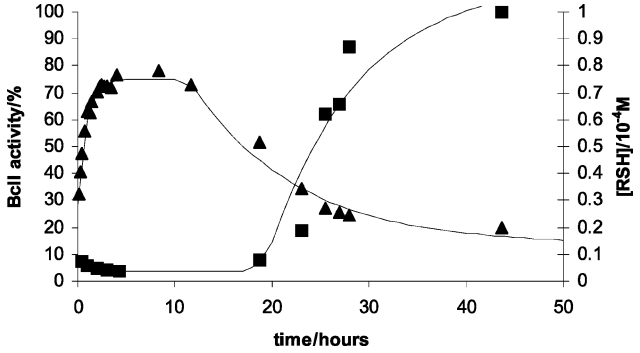

FIGURE 3: Variation of the thiol concentration (▲) as a function of the time the cephalexin intramolecular aminolysis product (**9**) (10^{-2} M) has been incubated in 0.1 M sodium hydroxide and then diluted 100-fold into 0.1 M MOPS, pH 7.0. Variation of BcII activity (■), after adding 10^{-4} M cephalexin intramolecular aminolysis product (**9**), as a function of the time compound **9** has been incuated in 0.1 M sodium hydroxide. The solid lines represent the sequential first-order fit of the experimental data points. Standard deviations are below 10%.

derivatives were present as the inhibitor. Furthermore, these products are derived from a mixture of the hydrolysis product (**10**) and the intramolecular aminolysis product (**9**). Solutions of **9** and **10**, 10^{-2} M, were incubated in 0.1 M NaOH at 30 °C, and, as described above, after different incubation times, the UV absorbance of the solutions was monitored and their effect on BcII activity measured. In addition, the thiol concentration in the assay cell was determined using Ellman's reagent (*44*). That inhibition is due to the formation of a thiol from the degradation products was demonstrated by a similar time response to Ellman's reagent, the amount of enzyme inhibition being proportional to the amount of thiol present. Maximum inhibition of BcII occurs at a point corresponding to maximum thiol concentration (>80%) derived from **9** and **10**, which is reached faster (4 h) for the intramolecular aminolysis product (**9**) (Figure 3) than from the hydrolysis product (23 h) (**10**) (Figure 4). This may be due to the diazadione side chain giving a more stable intermediate compared with a carboxylate anion. The recovery of enzyme activity is due to the loss of the thiol which is removed by a pH-dependent reaction. For example, if the thiol generated from cephalexin (**8**) by incubation in 0.1 M sodium hydroxide for 20 h is transferred to solutions of different pH, the rate of recovery of enzyme activity varies with pH (Figure 5). If the thiol solution is kept at pH 13, then it remains an effective inhibitor for BcII for more than 2 days because the thiol is stable under these conditions, although it is eventually removed after about 1 week by oxidation following hydrolysis of the imine. Conversely, at pH 7 and 2 the inhibitory properties are lost as the thiol is oxidized over 1−2 days.

These observations are compatible with the reactions outlined in Scheme 6. It is known that the hydrolysis products of cephalosporins undergo epimerization and degradation *(48)*. Epimerization at C6 involves ring opening of the dihydrothiazine to generate a thiol intermediate (*47*). Two thiols (**11** or **12** and **13** or **14**) can be potentially generated by dihydrothiazine ring opening which are a tautomeric equilibrium of imine and enamine. The thiol iminium ion (**13** or **14**) is formed directly by unimolecular ring opening whereas the thiol enamine (**11** or **12**) is the result of base-catalyzed elimination across C7−C6 and ring opening (Scheme 6). It is presumably one of the thiols (**11** or **12**, or **13** or **14**) shown in Scheme 6 that causes inhibition of the metallo-β-lactamase by coordination to the active site zinc, as has been suggested for other thiols (*29*). The iminium ion (**13**, **14**) is slowly hydrolyzed to the corresponding aldehyde at C6 (**17** or **18**) and the thiol enamine (**19**). The latter can also undergo further hydrolysis to the α-keto-δ-thiocarboxylic acid (**20**), which can form the thiolactone (**21**)(*46*) or be oxidized to the disulfide (**22**), thus removing the thiol.

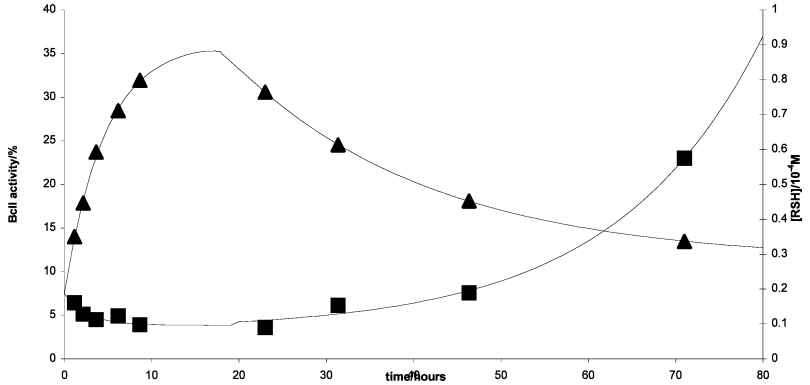

FIGURE 4: Variation of the thiol concentration (▲) as a function of the time the cephalexin hydrolysis product (**10**) (10^{-2} M) has been incubated in 0.1 M sodium hydroxide and then diluted 100-fold into 0.1 M MOPS, pH 7.0. Variation of BcII activity (■), after adding 10^{-4} M cephalexin hydrolysis product (**10**), as a function of the time compound **10** sodium hydroxide. The solid lines represent the sequential first-order fit of the experimental data points. Standard deviations are below 10%.

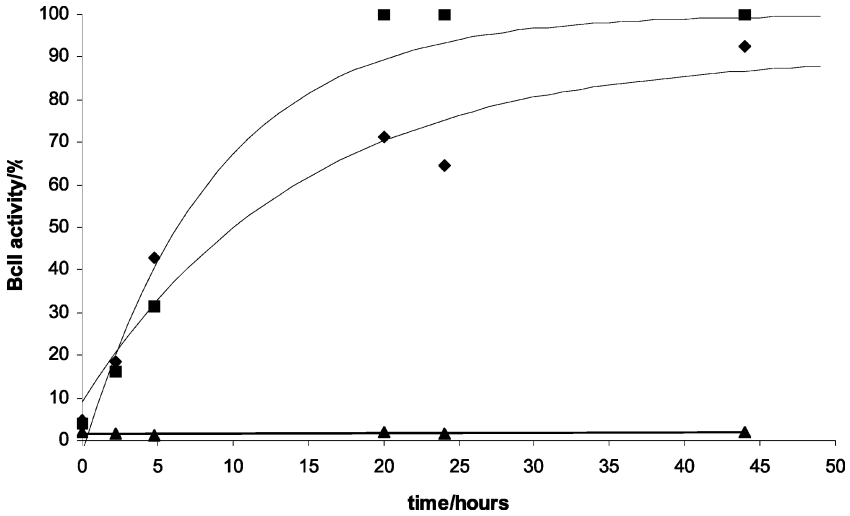

FIGURE 5: Variation of BcII activity, after adding 10^{-4} M cephalexin degradation product that has been kept for 20 h in 0.1 M sodium hydroxide, as a function of the time it has then been incubated at pH 2 (◆), pH 7 (■), and pH 13 (▲); time 0 corresponds to the incubation of cephalexin (10^{-2} M) in 0.1 M sodium hydroxide for 20 h. The solid lines represent the first-order fit of the experimental data points. Standard deviations are below 10%.

Scheme 6

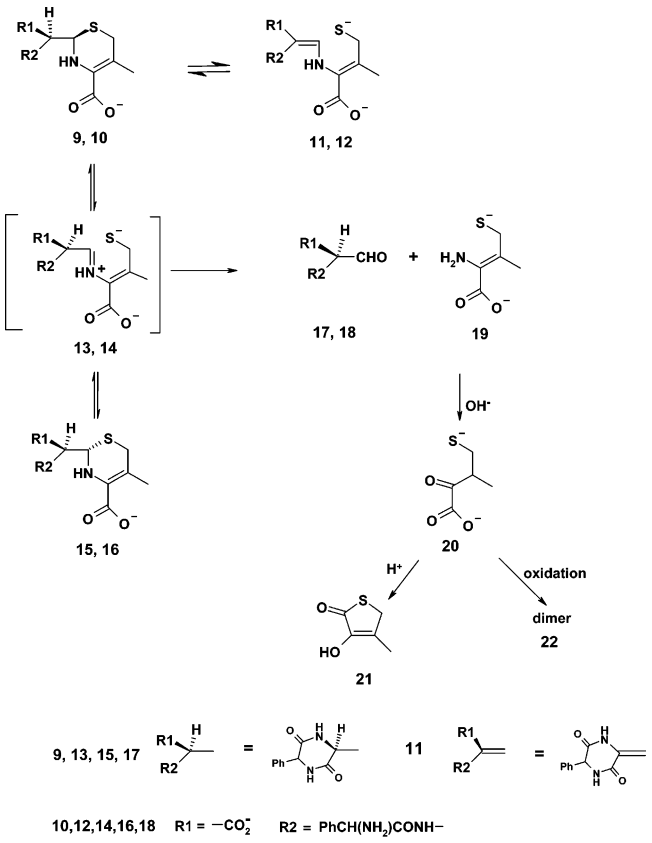

To distinguish which of the possible thiols present in the system **11** or **12**, **13** or **14**, or **19** or **20** (Scheme 6) is causing inhibition, ^{1}H NMR studies were carried under the same condition used to generate the thiol inhibitors. When cephalexin hydrolysis product **10**, obtained enzymatically, is incubated in pD 12.4, the main components after 30 h are **10** and its C6 epimer **16**. The hydrogens H6 and H7 of **10** and **16** appear as doublets, indicating that there has been no deuterium exchange. Ring opening and thiol formation as a result of proton abstraction at C7 and elimination across C7 and C6 would generate an enamine **12**. Subsequent ring closure to give the C6 epimer requires reprotonation at C7

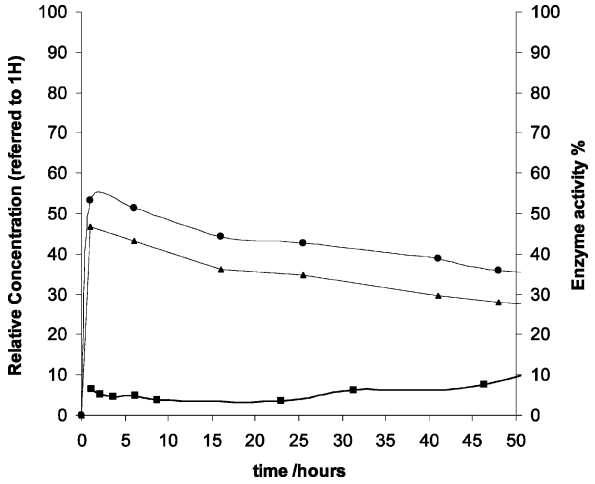

FIGURE 6: Plot of the evolution of cephalexin degradation products, the acid (●, **10**) and its epimer (▲, **16**), at pD 12.4 and 30 °C followed by ^{1}H NMR and BcII activity (■) as a function of time at the same conditions. The solid lines represent the first-order fit of the experimental data points. Standard deviations are below 10%.

leading to H−D exchange. Consequently, it appears that epimerization occurs through iminium ion formation (**14**) and that the ring closure occurs faster than enamine−imine tautomerization. This suggests that thiol imine **14** is present in solution, and although not present in high concentrations it is sufficiently long-lived for it to be trapped by the metalloenzyme and by Ellman's reagent.

Time-dependent ^{1}H NMR studies of the degradation of the cephalexin hydrolysis product (**10**) at pD 12.4 show that maximum epimerization at C6 occurs within 1 h (Figure 6), and the epimers are very stable, in agreement with the inhibition profile. As no other significant breakdown products were detected over a period of 30 h, it appears that derivatives such as **12**, **19**, or **20** are not present in solution during the maximum inhibition period. The thiol responsible for BcII inhibition is therefore most likely the intermediate **14**. However, the intermediate **14** in solution could not be detected directly by ^{1}H NMR, suggesting that its steady-state concentration is less than 10% of the total degradation product. Consequently, the real K_i value for the competitive

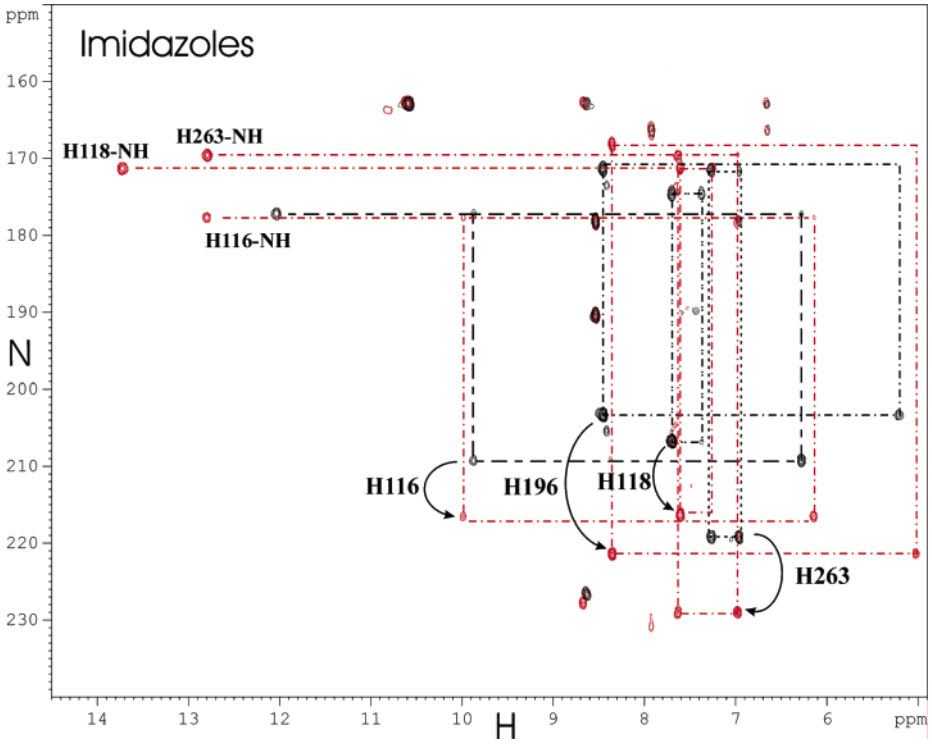

FIGURE 7: $^{1}H-^{15}N$ HMQC spectra optimized for imidazole observation of BcII in the presence and absence of cephalexin degradation products at pH 7.1. The cross-peaks are shown in black for the spectrum of the enzyme alone and in red for that of the complex with cephalexine degradation products. The four metal-bound imidazoles are labeled: His116, His118, and His196 in site I and His263 in site II. The three observed imidazole NH are labeled: His116-NH, His118-NH, and His263-NH.

inhibition of BcII with the thiol intermediate **14** is less than 40 nM.

^{15}N NMR studies of the complex between ^{15}N-labeled BcII and the cephalexin degradation product, obtained in 0.1 M NaOH, show that binding of the inhibitor affects substantially both zinc binding sites in the enzyme. The resonances of all the unprotonated imidazole nitrogens involved in zinc binding (Nϵ for His116 and His196 and Nδ for His118 of the histidines in site I, and Nϵ for His263 of the histidine in site II) show large downfield shifts: 8 ppm for His116; 18 ppm for His196, 9 ppm for His118, and 10.5 ppm for His263, much larger than those reported previously for the complex between BcII and (*R*/*S*)-thiomandelate (*33*). It appears that the thiol of the degradation product binds to the zinc ion, which in turn perturbs the metal-bound histidines.

NMR experiments $^{1}H-^{15}N$ HMQC optimized for observation of the long-range couplings in the imidazole ring (*26*) allow one to correlate two nitrogens with the two (C)H protons within each imidazole. The imidazole resonances of the metal binding histidine residues (His116, His118, and His196 in site I, His263 in site II), have been assigned to individual residues for the free enzyme (*26*). Whereas there are changes in ^{15}N and (C)H chemical shifts on inhibitor binding, the pattern of connectivities in the HMQC spectrum (Figure 7) permits the assignment of the imidazole resonances in the spectrum of the cephalexin degradation products as done previously for (*R*)- and (*S*)-thiomandelic acid complexes by comparison with the spectrum of the free enzyme (*33*). The observation by NMR of both the imidazole (N)H resonance and the imidazole N(C)H correlation in aqueous solution is rare because of the fast chemical exchange with water protons. These signals are observed only for imidazoles that are protected from the bulk water as in a hydrophobic core or for imidazoles that are involved in very strong hydrogen bonds (*49*). Of the seven histidines of BcII, all four that chelate the two metals (H116, H118, H196, and H263) have observable imidazole signals. These signals disappear when the metals are removed with EDTA.

In the case of the monocadmium BcII, none of the metal-bound imidazole signals can be observed because of the fast chemical exchange caused by the "jumping" metal ion between the two sites (*26*). Therefore, the observation by $^{1}H-^{15}N$ HMQC of the four active site imidazoles involved in metal binding is only possible for the dimetallic enzyme. In the present situation with cephalexin degradation products, the four metal-bound histidine imidazole signals are observed and are the only imidazole signals affected by the presence of the inhibitor. This situation is very similar to that observed with the inhibition by thiomandelate, which has been fully characterized by Cd, N, and H NMR as a dimetallic enzyme (*50*). There is therefore little doubt about the presence of two metal cations in the complex with cephalexin degradation products. In the case of the monocadmium BcII, the inhibitor (*R*)-thiomandelate induces a very strong positive cooperativity for binding the second cadmium cation, but this has not been explored with the thiol from cephalexin.

The $^{1}H-^{15}N$ HMQC experiments show that the four metal-bound imidazole nitrogens are more affected in the complex with the cephalexin thiol (Figure 7) than in the complex with (*R*)-thiomandelate (*33*). The backbone NH chemical shift differences between the complex and free enzyme for (*R*)-thiomandelate and cephalexin thiol show that both inhibitors affect the backbone the same way.

(ii) Cephaloridine and Cephalothin Degradation Products. Inhibition of BcII was also observed by the degradation products from cephaloridine (**23**) and cephalothin (**24**).

Scheme 7

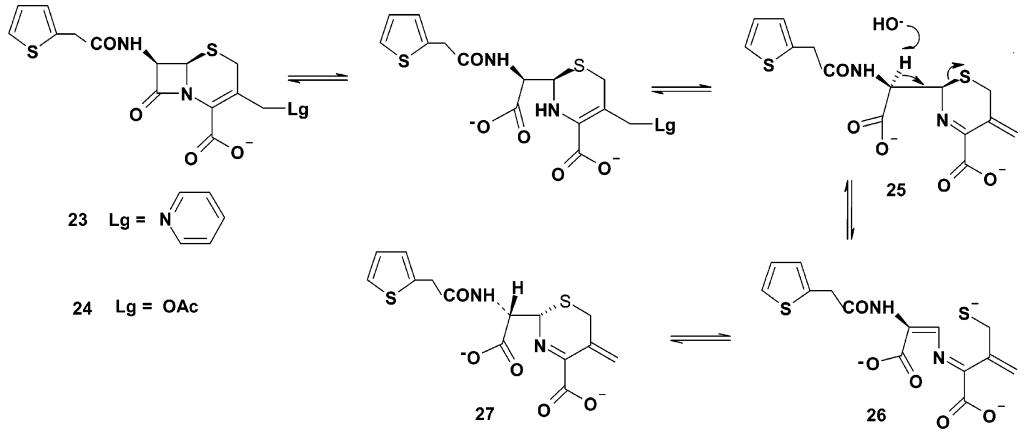

However, these antibiotics generated less effective inhibitors than that from cephalexin. Cephaloridine degradation products, generated by incubation of cephaloridine in 0.1 M sodium hydroxide, inhibit BcII with an apparent K_i of 35 μM, at $[Zn^{2+}] = 1$ μM, whereas those from cephalothin give a K_i of 45 μM, at $[Zn^{2+}] = 1$ μM.

Cephaloridine (**23**) and cephalothin (**24**) hydrolysis products differ from that derived from cephalexin because pyridine and acetate, respectively, at C3 are expelled to give the α,β-unsaturated imine **25** (Scheme 7) (*48*). Although, in this case, the imine **25** cannot readily undergo unimolecular ring opening to generate a thiol, because of generating an unstable carbocation at C6. However, C−S bond cleavage can occur by a slower process involving base-catalyzed elimination across C7−C6 to generate the conjugated imine **26** (Scheme 7) and as shown by the observation of deuterium exchange and epimerization at C7 (*47*).

The hydrolysis product from cephaloridine (**23**) (10^{-2} M), obtained enzymatically using P99 β-lactamase, was incubated in MOPS buffer at pH = 7.0, [I] = 1.0 M, $[Zn^{2+}] = 5 \times 10^{-5}$ M, in the presence of 3.24 μM BcII. At different incubation times, 10 μL aliquots of this solution were injected into 2 mL of MOPS buffer, and the enzyme activity was measured against a control. There was a reduction in activity to less than 10% (after 4 h 40 min), followed by a subsequent reactivation of the enzyme after about 1 day (Figure 8). A similar inhibition profile was obtained if the cephaloridine hydrolysis product was incubated under the same conditions as above, but without the enzyme present in the incubation mixture. The incubation mixture was also tested for the presence of thiol using Ellman's reagent, which indicated that the total amount of thiol present in the assay cell, at the time corresponding to maximum inhibition, is about 4.6 μM, representing 9% of the total original cephaloridine concentration.

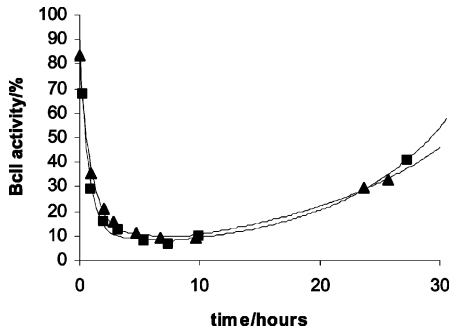

FIGURE 8: Variation of BcII activity as a function of the time BcII has been incubated with 10^{-2} M cephaloridine (▲) or cephalothin (■) hydrolysis product, in 0.1 M MOPS, pH 7.0. The solid lines represent the sequential first-order fit of the experimental data points. Standard deviations are below 10%.

Similar behavior was seen using the hydrolysis product derived from cephalothin, obtained enzymatically with P99 β-lactamase, under the same conditions as above but using 8.11 μM BcII. The minimum enzyme activity, 7%, was attained after 7 h 20 min of incubation of the hydrolysis product at pH 7.0, in the presence of the enzyme (Figure 8). When the hydrolysis product was incubated at pH = 7.0 in absence of the enzyme, its activity was reduced to only 28%.

In contrast to these observations, the cephalexin hydrolysis product incubated at pH 7.0 does not show any significant inhibition of BcII, due probably to the reduced stability of intermediate **14** in neutral pH, compared with the neutral imine at higher pH. With cephalexin, inhibition only occurs when the hydrolysis product has been incubated in 0.1 M sodium hydroxide, as described previously.

Scheme 8 shows the main degradation pathways for cephaloridine and cephalothin at pD = 7.4 and 30 °C. Time-dependent product analysis by ^{1}H NMR correlates well with the results obtained from the kinetic inhibition experiments. The dimer **30** of the ketothiol **28** was detected soon after the hydrolysis products from cephaloridine and cephalothin were formed, and it was therefore possible that **28** was responsible for the inhibition of BcII. However, a kinetic analysis of the evolution of the NMR signals indicates that the rate of oxidation of **28** to **30** is too fast to correspond to the rate of recovery of enzyme activity. The dimer **30** could be reduced to the thiol **28** by the addition of DTT to the solution of the hydrolysis products after 20 h of incubation at pD = 7.4. The signals of **30** broadened and shifted upfield, indicating that the disulfide bridge was broken and the new signals were due to the formation of **28**. When Ellman's reagent was added after the same time period, there was no signal shift, which would be expected if the signals were due to **26** or **28** rather than **30**.

Further evidence for the degradation pathway of cephaloridine and cephalothin following that shown in Scheme 8 comes from experiments carried out under the same conditions as those above but in the presence of Ellman's reagent. Ellman's reagent traps the intermediate thiol **26** forming a

Scheme 8

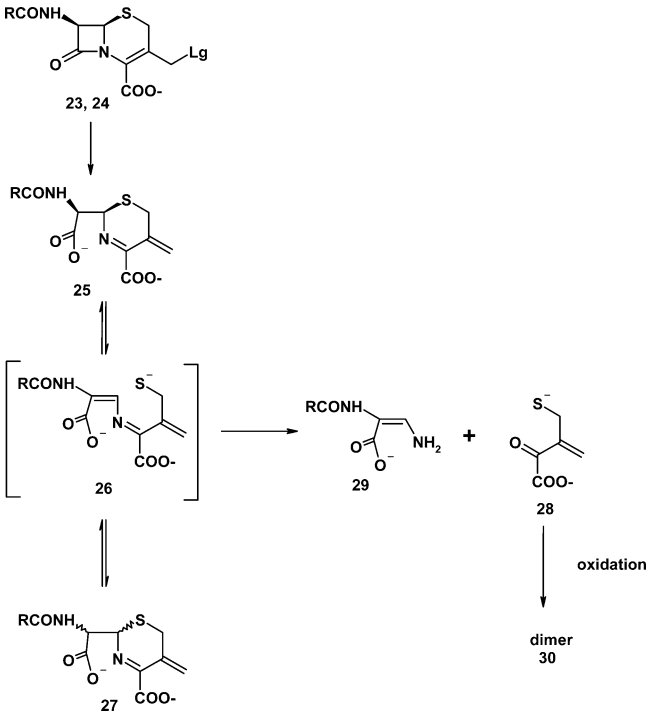

disulfide bridge and so prevents ring closure and epimerization to give **27**. No ^{1}H NMR signals corresponding to the C6 epimer **27** appear, and those corresponding to the C2 protons of intermediate **26** are shifted slightly and appear as an AB system, indicative of magnetic nonequivalance in the Ellman disulfide adduct. A similar situation occurs with the C2 proton signals of the dimer **30**, which, after the addition of DTT, are shifted back to their original positions and multiplicity.

Plots of the integrals of compounds shown in Scheme 8 against reaction time (Figure 9) demonstrate that the concentration of intermediate **26** builds up at the same rate as that for the loss of enzyme activity. The time at which **26** reaches its highest concentration matches the time at which the enzyme shows its greatest inhibition. Furthermore, as the concentration of **26** slowly decreases, the enzyme activity recovers at a similar rate.

If the hydrolysis products of cephalexin, cephaloridine, and cephalothin (10^{-4} M), obtained enzymatically using P99, respectively, are reacted with Ellman's reagent (10^{-4} M) in MOPS buffer (0.1 M, pH 7.0, [Zn] = 5×10^{-5} M, [I] = 1.0 M), the slow increase in absorbance at 412 nm, corresponding to formation of a thiol, reaches a maximum after about 15 h. The amount of thiol formed corresponds to 67% of the total cephalexin hydrolysis product concentration but to only 15% and 9% of the total cephalothin and cephaloridine hydrolysis product concentrations, respectively.

When the hydrolysis products of cephaloridine and cephalothin are incubated with the enzyme, there are higher levels of inhibition compared with no enzyme present. This could be explained either by a slow binding between the enzyme and the inhibitor or by the fact that the enzyme stabilizes the active form of the inhibitor by favorable binding interactions. To distinguish between the two mechanisms of inhibition, the conditions used to monitor the enzyme activity were modified so that a slow interaction between the enzyme and the inhibitor would become apparent (Scheme 4) (*43*). With lower enzyme and higher substrate concentrations and in the presence of different concentrations of cephalothin hydrolysis product, an initial "burst" of the rate ν_0 was followed by a progressive decay to a steady-state rate ν_s (Figure 10). Both ν_0 and ν_s were found to decrease with increasing inhibitor concentration, and reaching the steady-state rate was faster at high inhibitor concentrations, in agreement with the model in Scheme 4 and to eqs 2−4.

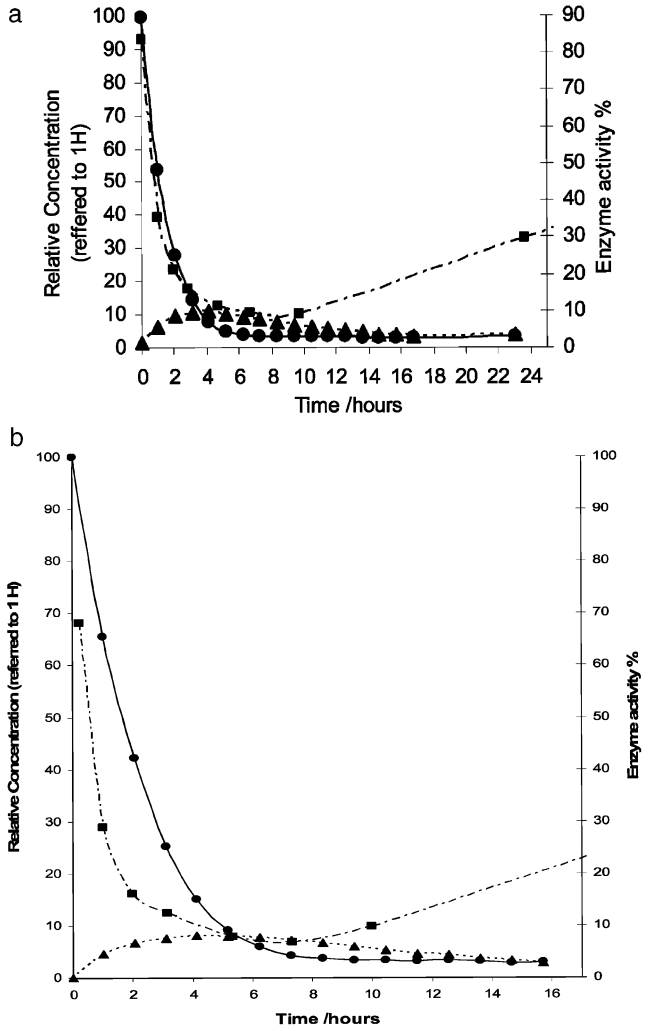

FIGURE 9: Plot of the evolution of (a) cephaloridine and (b) cephalothin degradation products, the acid (●, **25**) and the intermediate (▲, **26**), at pD 7.4 and 30 °C followed by ^{1}H NMR and BcII activity (■) as a function of time at the same conditions. The lines represent the sequential first-order fit of the experimental data points. Standard deviations are below 10%.

The parameters depicted in Scheme 4 are presented in Table 1 and were determined as described in the Experimental Procedures. The inhibitor concentration used in the calculations was 10% of the total cephalothin degradation product added, as determined by ^{1}H NMR (Figure 9b) for intermediate **26**. A good fit of the data (Figure 10, solid lines) was obtained using these parameters, suggesting that intermediate **26** is a slow binding inhibitor of BcII. Also, because the concentration required for detectable inhibition is much greater (2−3 orders of magnitude) than that of the enzyme, the thiol intermediate **26** is not a tight binding inhibitor of BcII.

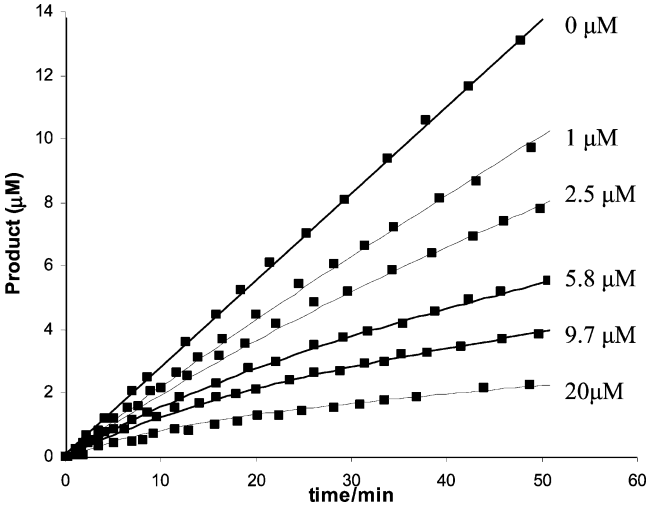

FIGURE 10: Inhibition of BcII as a function of the concentration of thiol intermediate **26**. All assays are performed in 0.1 M MOPS buffer, pH 7.0, $I = 1$ M, $[Zn^{2+}] = 5 \times 10^{-5}$ M. The concentrations of the substrate and enzyme were 75 μM and 0.25 nM, respectively. The reaction was initiated by addition of enzyme to a mixture of substrate and thiol intermediate **26** at the concentration indicated in the figure. The filled squares represent the experimental data points and the solid lines, the fit of the progress curves to the eq 1, using the v_0, v_s, and k values calculated from eqs 2−4 with the parameters in Table 1. Standard deviations are below 10%.

Table 1: Parameters for Inhibition of the BcII-Catalyzed Hydrolysis of Nitrocefin by Thiol Intermediate **26**[a]

parameter	calcd value	parameter	calcd value
[E] (nM)	0.25	K_i (μM)	3.74
[S] (μM)	75	K_i* (μM)	0.5
K_m (μM)	21.1	k_4 ($\times 10^4$ s^{-1})	19.5
V_{max} (nM/s^{-1})	5.16	k_{-4} ($\times 10^4$ s^{-1})	3.01

[a] Standard deviations are below 10%.

The fact that, under the same conditions, the thiol intermediate **14** produced from the degradation of cephalexin in 0.1 M NaOH does not show slow binding inhibition of BcII suggests that the slow step may be due to the lower degree of flexibility in the three conjugated double bond systems in the thiol intermediate **26** compared with the two conjugated double bond system in the thiol intermediate **14**. The slow binding inhibition of IMP1 and BcII by thiols has been reported previously (*51*). It was found that the slow binding character is significant for neutral thiols but decreases on introducing anionic groups into the molecule, with decreasing distance between the thiol and anionic substituent. The molecular mechanism proposed for the slow interaction involves the rearrangement of the enzyme, following the rupture of the μ-OH bridge upon coordination of the thiol to the Zn(2), or the replacement of the μ-OH bridge by the μ-SR bridge. The rate constants k_4 and k_{-4} for the rearrangement of the EI complex for IMP1 (*51*) and benzylmercaptan are 16- and 45-fold, respectively, greater than those for BcII with the thiol imine **26**. The slower reaction in the latter case is indicative of the slow step being a rearrangement of the thiol intermediate **26** in the enzyme active site, rather than the enzyme rearrangement or the nucleophilic substitution of OH by SR proposed for neutral thiols.

The recovery of enzyme activity of BcII after it has been incubated with the inhibitor does not return to 100%, possibly because, after long incubation times, a subsequent oxidation occurs between the thiol groups of the inhibitor and the cysteine residue in the enzyme active site, with the formation of a disulfide bond which irreversibly inactivates the enzyme.

Interestingly, under the same conditions, the benzylpenicilloic acid generated from benzylpenicillin does not give any degradation products that cause inhibition up to 1 mM. This is presumably because the analogous ring-opened thiazolidine (Scheme 2) is less stable and cannot be trapped, even though it is known that penicillin derivatives also undergo epimerization at C5 and C6 (*41*, *52*). We make no claims about the physiological relevance of our observations, but the data presented here do raise the possibility that suitably substituted cephalosporins could be used for inhibiting both transpeptidases and metallo-β-lactamases.

REFERENCES

1. Frère, J. M. (1995) Beta-lactamases and bacterial resistance to antibiotics, *Mol. Microbiol. 16*, 385−395.
2. Wang, Z., Fast, W., Valentine, A. M., and Benkovic, S. J. (1999) Metallo-β-lactamase: structure and function, *Curr. Opin. Chem. Biol. 3*, 614−622.
3. Laraki, N., Franceschini, N., Rossolini, G. M., Santucci, P., Meunier, C., de Pauw, E., Amicosante, G., Frère, J. M., and Galleni, M. (1999) Biochemical characterisation of the *Pseudomonas aeruginosa* 101/1477 metallo-β-lactamase IMP-1 produced by *Escherichia coli*, *Antimicrob. Agents Chemother. 43*, 902−906; Payne, D. J. (1993) Metallo-beta-lactamases—a new therapeutic challenge, *J. Med. Microbiol. 39*, 93−99.
4. Galleni, M., Lamotte-Brasseur, J., Rossolini, G. M., Spencer, J., Dideberg, O., and Frère, J. M. (2001) Standard numbering scheme for class B β-lactamases, *Antimicrob. Agents Chemother. 45*, 660−663.
5. Fabiane, S. M., Sohi, M. K., Wan, T., Payne, D. J., Bateson, J. H., Mitchell, T., and Sutton, B. J. (1998) Crystal structure of the zinc-dependent β-lactamase from *Bacillus cereus* at 1.9 Å resolution: binuclear active site with features of a mononuclear enzyme, *Biochemistry 37*, 12404−12411.
6. Orellano, E. G., Girardini, J. E., Cricco, J. A., Ceccarelli, E. A., and Vila, A. J. (1998) Spectroscopic characterization of a binuclear metal site in *Bacillus cereus* β-lactamase II, *Biochemistry 37*, 10173−10180; Paul-Soto, R., Bauer, R., Frère, J. M., Galleni, M., Meyer-Klaucke, W., Nolting, H., Rossolini, G. M., de Seny, D., Hernandez-Valladares, M., Zeppezauer, M., and Adolph, H. W. (1999) Mono- and binuclear Zn^{2+}-beta-lactamase. Role of the conserved cysteine in the catalytic mechanism, *J. Biol. Chem. 274*, 13242−13249.
7. Concha, N. O., Rasmussen, B. A., Bush, K., and Herzberg, O. (1996) Crystal structure of the wide-spectrum binuclear zinc β-lactamase from Bacteroides fragilis, *Structure 4*, 823−836.
8. Paul-Soto, R., Hernadez-Valladares, M., Galleni, M., Bauer, R., Zeppezauer, M., Frère, J. M., and Adolph, H. W. (1998) Mono- and binuclear Zn-beta-lactamase from Bacteroides fragilis: catalytic and structural roles of the zinc ions, *FEBS Lett. 438*, 137−140; Yang, Y., Keeney, D., Tang, X., Canfield, N., and Rasmussen, B. A. (1999) Kinetic properties and metal content of the metallo-β-lactamase CcrA harboring selective amino acid substitutions, *J. Biol. Chem. 274*, 15706−15711.
9. Wang, Z., Fast, W., and Benkovic, S. J. (1999) On the mechanism of the *Bacteroides fragilis* metallo-β-lactamase, *Biochemistry 38*, 10013−10023.
10. Laraki, N., Franceschini, N., Rossolini, G. M., Santucci, P., Meunier, C., de Pauw, E., Amicosante, G., Frère, J. M., and Galleni, M. (1999) Biochemical characterisation of the *Pseudomonas aeruginosa* 101/1477 metallo-β-lactamase IMP-1 produced by *Escherichia coli*, *Antimicrob. Agents Chemother. 43*, 902−906; Haruta, S., Yamaguchi, H., Yamamoto, E. T., Eriguchi, Y., Nukaga, M., O'Hara, K., and Sawai, T. (2000) Functional analysis of the active site of a metallo-β-lactamase proliferating in Japan, *Antimicrob. Agents Chemother. 44*, 2304−2309.
11. Concha, N. O., Janson, C. A., Rowling, P., Pearson, S., Cheever, C. A., Clarke, B. P., Lewis, C., Galleni, M., Frère, J. M., Payne, D. J., Bateson, J. H., and Abdel-Meguid, S. S. (2000) Crystal structure of the IMP-1 metallo β-lactamase from *Pseudomonas aeruginosa* and its complex with a mercaptocarboxylate inhibi-

tor: binding determinants of a potent, broad-spectrum inhibitor, *Biochemistry 39*, 4288−4298.
12. Hernandez Valladares, M., Felici, A., Weber, G., Adolph, H. W., Zeppezauer, M., Rossolini, G. M., Amicosante, G., Frère, J. M., and Galleni, M. (1997) Zn(II) dependence of the *Aeromonas* hydrophila AE036 metallo-β-lactamase activity and stability, *Biochemistry 36*, 11534−11541.
13. Crowder, M. W., Walsh, T. R., Banovic, L., Pettit, M., and Spencer, J. (1998) Overexpression, purification, and characterization of the cloned metallo-β-lactamase (L1) from *Stenotrophomonas maltophilia*, *Antimicrob. Agents Chemother. 42*, 921−926.
14. Mercuri, P. S., Bouillenne, F., Boschi, L., Lamotte-Brasseur, J., Amicosante, G., Devreese, B., van Beeumen, J., Frère, J. M., Rossolini, G. M., and Galleni, M. (2001) Biochemical characterization of the FEZ-1 metallo-β-lactamase of *Legionella gormanii* ATCC 33297T produced in *Escherichia coli*, *Antimicrob. Agents Chemother. 45*, 1254−1262.
15. Carfi, A., Duee, E., Galleni, M., Frère, J. M., and Dideberg, O. (1998) 1.85 Å resolution structure of the zinc(II) β-lactamase from *Bacillus cereus*, *Acta Crystallogr., Sect. D: Biol. Crystallogr. 54*, 313−323.
16. Carfi, A., Duee, E., Paul-Soto, R., Galleni, M., Frère, J. M., and Dideberg, O. (1998) X-ray structure of the ZnII β-lactamase from *Bacteroides fragilis* in an orthorhombic crystal form, *Acta Crystallogr., Sect. D: Biol. Crystallogr. 54*, 45−57.
17. Ullah, J. H., Walsh, T. R., Taylor, I. A., Emery, D. C., Verma, C. S., Gamblin, S. J., and Spencer, J. (1998) The crystal structure of the L1 metallo-β-lactamase from *Stenotrophomonas maltophilia* at 1.7 Å resolution, *J. Mol. Biol. 284*, 125−136.
18. García-Sáez, P., Mercuri, S., Papamicael, C., Kahn, R., Frère, J. M., Galleni, M., Rossolini, G. M., and Dideberg, O. (2003) Three-dimensional structure of FEZ-1, a monomeric subclass B3 metallo-β-lactamase from *Fluoribacter gormanii*, in native form and in complex with D-captopril, *J. Mol. Biol. 325*, 651−660.
19. Garau, G., Bebrone, C., Anne, C., Galleni, M., Frere, J.-M., and Dideberg, O. (2005) A metallo-β-lactamase in action: crystal structure of the monozinc carbapenemase CphA and its complex with biapenem, *J. Mol. Biol. 345*, 785−795.
20. Garcia-Saez, I., Hopkins, J., Papamicael, C., Franceschini, N., Amicosante, G., Rossolini, G. M., Galleni, M., Frère, J. M., and Dideberg, O. (2003) The 1.5-Å Structure of *Chryseobacterium meningosepticum* zinc β-lactamase in complex with the inhibitor, D-Captopril, *J. Biol. Chem. 278*, 23868−23873.
21. Fitzgerald, P. M., Wu, J. K., and Toney, J. H. (1998) Unanticipated inhibition of the metallo-β-lactamase from *Bacteroides fragilis* by 4-morpholineethanesulfonic acid (MES): a crystallographic study at 1.85-Å resolution, *Biochemistry 37*, 6791−6800; Concha, N. O., Rasmussen, B. A., Bush, K., and Herzberg, O. (1997) Crystal structure of the cadmium- and mercury-substituted metallo-beta-lactamase from *Bacteroides fragilis*, *Protein Sci. 6*, 2671−2676; Toney, J. H., Fitzgerald, P. M., Grover-Sharma, N., Olson, S. H., May, W. J., Sundelof, J. G., Vanderwall, D. E., Cleary, K. A., Grant, S. K., Wu, J. K., Kozarich, J. W., Pompliano, D. L., and Hammond, G. G. (1998) Antibiotic sensitization using biphenyl tetrazoles as potent inhibitors of *Bacteroides fragilis* metallo-β-lactamase, *Chem. Biol. 5*, 185−196.
22. Carfi, A., Pares, S., Duee, E., Galleni, M., Duez, C., Frère, J. M., and Dideberg, O. (1995) The 3-D structure of a zinc metallo-β-lactamase from *Bacillus cereus* reveals a new type of protein fold, *EMBO J. 14*, 4914−4921.
23. Paul-Soto, R., Zeppezauer, M., Adolph, H. W., Galleni, M., Frère, J. M., Carfi, A., Dideberg, O., Wouter, J., Hemmingsen, L., and Bauer, R. (1999) Preference of Cd(II) and Zn(II) for the two metal sites in *Bacillus cereus* β-lactamase II: a perturbed angular correlation of γ-rays (PAC) spectroscopy study, *Biochemistry 38*, 16500−16506.
24. Toney, J. H., Hammond, G. G., Fitzgerald, P. M., Sharma, N., Balkovec, J. M., Rouen, G. P., Olson, S. H., Hammond, M. L., Greenlee, M. L., and Gao, Y. D. (2001) Succinic acids as potent inhibitors of plasmid-borne IMP-1 metallo-β-lactamase, *J. Biol. Chem. 276*, 31913−31918.
25. Prosperi-Meys, C., Wouters, J., Galleni, M., and Lamotte-Brasseur, J. (2001) Substrate binding and catalytic mechanism of class B β-lactamases: a molecular modelling study, *Cell. Mol. Life Sci. 58*, 2136−2143.
26. Hemmingsen, L., Damblon, C., Antony, J., Jensen, M., Adolph, H. W., Wommer, S., Roberts, G. C. K., and Bauer, R. (2001) Dynamics of mononuclear cadmium β-lactamase revealed by the combination of NMR and PAC spectroscopy, *J. Am. Chem. Soc. 123*, 10329−10335; Damblon, C., Prosperi, C., Lian, L. Y., Barsukov, I., Paul-Soto, R., Galleni, M., Frère, J. M., and Roberts, G. C. K. (1999) ^{1}H-^{15}N HMQC for the identification of metal-bound histidines in ^{113}Cd-substituted *Bacillus cereus* zinc β-lactamase, *J. Am. Chem. Soc. 121*, 11575−11576.
27. Walter, M. W., Felici, A., Galleni, M., Paul-Soto, R., Adlington, R. M., Baldwin, J. E., Frère, J. M., Golobov, M., and Schofield, C. J. (1996) Trifluoromethyl alcohol and ketone inhibitors of metallo-β-lactamases, *Bioorg. Med. Chem. Lett. 6*, 2455−2458.
28. Walter, M. W., Hernandez-Valladares, M., Adlington, R. M., Amicosante, G., Baldwin, J. E., Frère, J. M., Galleni, M., Rossolini, G. M., and Schofield, C. J. (1999) Hydroxamate inhibitors of *Aeromonas hydrophila* AE036 metallo-β-lactamase, *Bioorg. Chem. 27*, 35−40.
29. Arawaka, Y., Shibata, N., Shibayama, K., Kurokawa, H., Yagi, T., Fujiwara, H., and Goto, M. (2000) Convenient test for screening metallo-β-lactamase-producing gram-negative bacteria by using thiol compounds, *J. Clin. Microbiol. 38*, 40−43.
30. Bounaga, S., Laws, A. P., Galleni, M., and Page, M. I. (1998) The mechanism of catalysis and the inhibition of the *Bacillus cereus* zinc-dependent β-lactamase, *Biochem J. 331*, 703−711.
31. Goto, M., Takahashi, T., Yamashita, F., Koreeda, A., Mori, H., Ohta, M., and Arakawa, Y. (1997) Inhibition of the metallo-β-lactamase produced from *Serratia marcescens* by thiol compounds, *Biol. Pharm. Bull. 20*, 1136−1140.
32. Greenlee, M. L., Laub, J. B., Balkovec, J. M., Hammond, M. L., Hammond, G. G., Pompliano, D. L., and Epstein-Toney, J. H. (1999) Synthesis and SAR of thioester and thiol inhibitors of IMP-1 metallo-β-lactamase, *Bioorg. Med. Chem. Lett. 9*, 2549−2554.
33. Mollard, C., Moali, C., Papamicael, C., Damblon, C., Vessilier, S., Amicosante, G., Schofield, C. J., Galleni, M., Frère, J. M., and Roberts, G. C. K. (2001) Thiomandelic acid, a broad-spectrum inhibitor of zinc β-lactamases: kinetic and spectroscopic studies, *Biol. Chem. 276*, 45015−45023.
34. Bounaga, S., Galleni, M., Laws, A. P., and Page, M. I (2001) Cysteinyl peptide inhibitors of *Bacillus cereus* zinc beta-lactamase, *Bioorg. Med. Chem. 9*, 503−510.
35. Hammond, G. G., Huber, J. L., Greenlee, M. L., Laub, J. B., Young, K., Silver, L. L., Balkovec, J. M., Pryor, K. D., Wu, J. K., Leiting, B., Pompliano, D. L., and Toney, J. H. (1999) Inhibition of IMP-1 metallo-β-lactamase and sensitisation of IMP-1-producing bacteria by thioester derivatives, *FEMS Microbiol. Lett. 179*, 289−296.
36. Payne, D. J., Bateson, J. H., Gasson, B. C., Proctor, D., Khushi, T., Farmer, T. H., Toldon, D. A., Bell, D., Skett, P. W., Marshall, A. C., Reid, R., Ghosez, L., Combret, Y., and Marchand-Brynaert, J. (1997) Inhibition of metallo-β-lactamases by a series of mercaptoacetic acid thiol ester derivatives, *Antimicrob. Agents Chemother. 41*, 135−140; Payne, D. J., Bateson, J. H., Gasson, B. C., Khushi, T., Proctor, D., Pearson, S. C., and Reid, R. (1997) Inhibition of metallo-β-lactamases by a series of thiol ester derivatives of mercapto-phenylacetic acid, *FEMS Microbiol. Lett. 157*, 171−175.
37. Toney, J. H., Fitzgerald, P. M., Grover-Sharma, N., Olson, S. H., May, W. J., Sundelof, J. G., Vanderwall, D. E., Cleary, K. A., Grant, S. K., Wu, J. K., Kozarich, J. W., Pompliano, D. L., and Hammond, G. G. (1998) Antibiotic sensitization using biphenyl tetrazoles as potent inhibitors of *Bacteroides fragilis* metallo-β-lactamase, *Chem. Biol. 5*, 185−196; Toney, J. H., Cleary, K. A., Hammond, G. G., Yuan, X., May, W. J., Hutchins, S. M., Ashton, W. T., and Vanderwall, D. E. (1999) Structure−activity relationships of biphenyl tetrazoles as metallo-β-lactamase inhibitors, *Bioorg. Med. Chem. Lett. 9*, 2741−2746.
38. Payne, D. J., Hueso-Rodríguez, J. A., Boyd, H., Concha, N. O., Janson, C. A., Gilpin, M., Bateson, J. H., Cheever, C., Niconovich, N. L., Pearson, S., Rittenhouse, S., Tew, D., Díez, E., Pérez, P., De La Fuente, J., Rees, M., and Rivera-Sagredo, A. (2002) Identification of a series of tricyclic natural products as potent broad-spectrum inhibitors of metallo-β-lactamases, *Antimicrob. Agents Chemother. 46*, 1880−1886.
39. Siemann, S., Evanoff, D. P., Marrone, L., Clarke, A. J., Viswantha, T., and Dimitrenko, G. I. (2002) N-arylsulfonyl hydrazones as inhibitors of IMP-1 metallo-β-lactamase, *Antimicrob. Agents Chemother. 46*, 2450−2457.
40. Wang, Z., and Benkovic, S. J. (1998) Purification, characterization, and kinetic studies of a soluble *Bacteroides fragilis* metallo-β-

lactamase that provides multiple antibiotic resistance, *J. Biol. Chem. 273*, 22402−22408.
41. Davies, A., M., and Page, M. I. (1985) Opening of the thiazolidine ring of penicillin derivatives, *J. Chem. Soc., Chem. Commun.*, 1702−1704.
42. Pratt, R. F., and Faraci, W. S. (1986) Direct observation by ^{1}H NMR of cephalosporoate intermediates in aqueous solution during the hydrazinolysis and β-lactamase-catalyzed hydrolysis of cephalosporins with 3′ leaving groups: kinetics and equilibria of the 3′ elimination reaction, *J. Am. Chem. Soc. 108*, 5328−5333; Bundgaard, H. (1977) Isolation and characterization of cephalexin degradation products formed in neutral aqueous solution, *Arch. Pharm. Chemi, Sci. Ed. 5*, 149−155. Vilanova, B., Frau, J., Donoso, J., Munoz, F., and Garcia Blanco, F. G. (1997) β-Lactamase-catalysed hydrolysis of cephalexin: evolution of the cephalosporoate intermediate, *J. Chem. Soc., Perkin Trans. 2*, 2439−2444.
43. Morrison, J. F., and Walsh, C., T. (1988) The behavior and significance of slow-binding enzyme inhibitors, *Adv. Enzymol. Relat. Areas Mol. Biol. 61*, 201−301.
44. Ellman, G. L. (1959) Tissue sulfhydryl groups, *Arch. Biochem. Biophys. 82*, 70−77; Riddles, P. W., Blakeley, R. L., and Zerner, B. (1979) Ellman's reagent: 5,5′-dithiobis(2-nitrobenzoic acid)—a reexamination, *Anal. Biochem. 94*, 75−81.
45. Bundgaard, H. (1976) Hydrolysis and intramolecular aminolysis of cephalexin and cephaloglycin in aqueous solution, *Arch. Pharm. Chemi, Sci. Ed. 4*, 25−43.
46. Dinner, A. (1977) Cephalosporin degradations, *J. Med. Chem. 20*, 963−965.
47. Vilanova, B., Munoz, F., Donoso, J., and Garcia Blanco, F. (1993) Degradation of cephaloridine on alkaline hydrolysis, *Helv. Chim. Acta 76*, 1619−1625.
48. Page, M. I. (1987) The mechanisms of reactions of β-lactam antibiotics, *Adv. Phys. Org. Chem. 23*, 165−270.
49. Pelton, J. G., Torchia, D. A., Meadow, N. D., and Roseman, S. (1993) Tautomeric states of the active-site histidines of phosphorylated and unphosphorylated III(Glc), a signal-transducing protein from *Escherichia coli*, using two-dimensional heteronuclear NMR techniques, *Protein Sci. 2*, 543−558.
50. Damblon, C., Jensen, M., Ababou, A., Barsukov, I., Papamicael, C., Schofield, C. J., Olsen, L., Bauer, R., and Roberts, G. C. (2003) The inhibitor thiomandelic acid binds to both metal ions in metallo-beta-lactamase and induces positive cooperativity in metal binding, *J. Biol. Chem. 278*, 29240−29251.
51. Siemann, S., Clarke, A. J., Viswanatha, T., and Dmitrienko, G. I. (2003) Thiols as classical and slow-binding inhibitors of IMP-1 and other binuclear metallo-β-lactamases, *Biochemistry 42*, 1673−1683.
52. Ghebre-Sellassie, I., Hem, S. L., and Knevel, A. M. (1984) Epimerization of benzylpenicilloic acid in alkaline media, *J. Pharm. Sci. 73*, 125−128.

BI050302J